Crystals **2012**, *2*, 1460-1482; doi:10.3390/cryst2041460

OPEN ACCESS

crystals

ISSN 2073-4352

www.mdpi.com/journal/crystals

Review

Pressure Effect on Organic Conductors

Keizo Murata [1,*], Keiichi Yokogawa [1], Sonachalam Arumugam [2] and Harukazu Yoshino [1]

[1] Graduate School of Science, Osaka City University, 3-3-138, Sugimoto, Sumiyoshi-ku, Osaka 558-8585, Japan; E-Mails: yokogawa@sci.osaka-cu.ac.jp (K.Y.); yoshino@sci.osaka-cu.ac.jp (H.Y.)

[2] Centre for High Pressure Research, Department of Physics, Bharathidasan University, Tiruchirappalli-620-024, India; E-Mail: sarumugam1963@yahoo.com

* Author to whom correspondence should be addressed; E-Mail: muratak@sci.osaka-cu.ac.jp; Tel.: +81-6-6605-2509; Fax: +81-6-6690-2710.

Received: 25 August 2012; in revised form: 17 September 2012 / Accepted: 21 September 2012 / Published: 23 October 2012

Abstract: Pressure is a powerful tool to unveil the profound nature of electronic properties in a variety of organic conductors. Starting from technology of high pressure, we plan to review what kind of physics or phenomena have previously been discussed.

Keywords: pressure; organic conductors; TTF-TCNQ; TSeF-TCNQ; HMTSF-TCNQ; $(TMTSF)_2X$; $(TMTTF)_2X$; α-$(BEDT\text{-}TTF)_2X$; β-$(BEDT\text{-}TTF)_2X$; κ-$(MeDH\text{-}TTP)_2AsF_6$; τ-type conductor

---

1. Introduction

It is true that the history of crystalline organic conductors is guided by the elaborate ideas and works generated by pressure experiments. The nature of a charge density wave (CDW) in tetrathiafulvalene-tetracyanoquinodimethane (TTF-TCNQ) is demonstrated by the smart analysis of conversion from conductivity, as a function of temperature at various pressures, to conductivity as a function of pressure at various temperatures [1]. By that analysis, the conductivity of CDW together with the fluctuation, as a collective motion, was well understood as phenomena at hand. Lots of trials of CDW suppression by pressure have been done from TTF-TCNQ through its family with the anticipation of superconductivity. Eventually, superconductivity was realized in $(TMTSF)_2PF_6$ by suppressing by the help of pressure the insulating phase, which was a spin density wave (SDW) instead

of a CDW, where TMTSF stands for tetramethyltetraselenafulvalene [2]. Field-Induced spin density waves are observed by tuning the pressure, where superconductivity is observed [3]. The lesson of the usefulness of pressure was further succeeded when high-T_c cuprate superconductors were discovered; pressure was the guiding tool in finding further materials [4]. Thus, the study of the pressure effect of the materials is already established as an indispensable experiment to find more. In this paper, we plan to review how the pressure effect contributed to various topics of the physics of organic conductors along descriptions of the technique of pressure.

2. Method of Pressure in Organic Conductors

The important role of the pressure as concerns solid state physics is already known for a long time. However, pressure as a tool has been developed mainly for inorganic materials at an early stage. Organic conductors can be classified into crystals and polymers. What we deal with in this paper is the organic crystals. Organic crystals are very fragile and weak mechanically. When a piston cylinder pressure cell of the clamp type is used and when the initial room temperature pressure is low, pressure becomes zero at low temperatures due to thermal contraction. In such cases, organic crystals are very likely to be broken (first problem). Voids might be produced in the pressure cell. The second problem is that organic crystals are seriously damaged at the instance of solidification of the pressure medium on cooling; for instance, if the medium is isopentane. Although the first one is a general problem for all pressure mediums and is inevitable except in the case of water, the second one due to solidification of the medium and can be solved by choosing a suitable pressure medium, which has a small volume difference at the instance of liquid-solid transition on cooling. To overcome this problem of damage to the sample on solidification by cooling, Daphne 7373 is developed [5,6]. The discontinuous drop in pressure through the solidification of Daphne 7373 is negligible, but is just observable by viewing the kink in the temperature dependence of resistance of pressure-sensitive crystals such as organic conductors. Actually, Daphne 7373 as a pressure medium was found to be a very suitable pressure medium for pressure works. Further, pressure drops or a change from room temperature to low (helium) temperature, is much smaller (typically ~0.15 GPa) than with Fluorinert 77/70 (typically ~0.5 GPa), for example. With these advantages, it was later found that Daphne 7373 is favorable even for inorganic materials. An example is the large amplitude of the de Haas van Alphen effect, whose temperature dependence determines the cyclotron mass [7,8].

In late 1990s, the pressure of the researcher's interest extended from 1 GPa to around 2–4 GPa region or up to 10 GPa. For instance, the topics of the quantum critical phenomena were discussed in 2–4 GPa region, the highest T_c-organic superconductivity [9], and 1D phase diagram of $(TMTTF)_2X$ were discussed in the 8–9 GPa region, where TMTTF is sulfur analog of TMTSF and is an abbreviation of tetramethyltetrathiafulvalene [10]. With these interests in the physics of the pressure region of the 3–4 GPa, a new piston cylinder cell other than the single walled BeCu cell was developed, which was the double-walled NiCrAl/BeCu cell. This new type of pressure cell achieved 4 GPa, in contrast to the single-walled BeCu cell with the maximum pressure of 1.5 GPa. By virtue of the stronger pressure cell, it was found that Daphne 7373 solidifies at 2.2 GPa [6,11], beyond which uniaxial compression is mixed with hydrostatic pressure. Another benefit of stronger pressure cell is that pressure values below 2.55 or 2.70 GPa became accurate for piston cylinder cell. There used to be

no easy fixed points of pressure above 0.363 GPa (or 1.08 GPa but dull) of NH_4F. Therefore, the stronger pressure allowed interpolation of pressure against the load of the press. To realize hydrostatic pressure beyond the solidification pressure (2.2 GPa) of Daphne 7373 with a stronger pressure cell, one (K/M) of the authors developed a new pressure medium, which solidified at 3.7 GPa. The new medium is named Daphne 7474 [11]. The value of 3.7 GPa can be raised almost linearly up to 6.7 GPa at 100 °C.

The high quality hydrostatic pressure is achieved by choosing either a good medium with a high solidification pressure or a good apparatus. Superconducting transition temperature (T_c) and its related pressure become apparently different either with a different pressure medium or with different apparatus. By using a pressure medium with low solidification pressure achieves superconductivity with apparently low (sometimes half of the intrinsic value of) pressure in the pnictides [12]. In other words, the higher the solidification of pressure medium, the better the quality of superconductivity is. But in the case of pnictides, high quality superconductivity requires higher pressure. On the other hand, as for apparatus choosing, cubic anvil gives different but more intrinsic values T_c and P_c from other apparatus for pnictide as well [13]. Cubic anvil fulfills this purpose by realizing high quality hydrostatic pressure. The high quality pressure plays an important role for anisotropic materials whose material property is sensitive to the compression along the specific direction.

Besides the efforts of seeking the high quality hydrostatic pressure, it is worth describing the technique of uniaxial compression. Since the organic conductors are low dimensional and the overlapping integrals between the adjacent molecules are very anisotropic, the uniaxial compression is a powerful tool to find out the dominant microscopic interaction, which is associated directly with the direction. Although the idea of uniaxial compression is attractive, the extremely fragile organic conductors have prevented its realization of uniaxial compression. The breakthrough was given by Campos, Brooks *et al.*, who buried the organic sample in an epoxy with already attached electrodes. Their method is to compress uniaxially the epoxy with a sample inside leaving two other sides of the epoxy block open, which allows expansion according to the Poisson's ratio in these two directions. This is called the *uniaxial stress* method [14]. Maesato and Kagoshima adopted the idea of immersing the samples into epoxy and extended the technique to piston cylinder. The uniaxial compression using a piston cylinder does not allow epoxy to expand two other directions. This effect is called the *uniaxial strain* method [15]. Maesato also proposed other method using the frozen oil by lowered temperature. The strain method is technically more advantageous and is free from the inevitable break of the epoxy block with the stress method. It is a matter of course that physics analysis becomes more simple when using the strain method, which deals only with the parameters of associated with one direction, whereas in stress method, with all directions. It should be noted that challenging work with direct X-ray observation under uniaxial pressure is coming out [16].

One should notice that the there is no ideal solid medium that is the same as the compressibility of the target material for the uniaxial strain method. At least, so long as the target material has an anisotropic compressibility, if the compressibility of the medium matches perfectly with that of the material along one direction, the compressibility of the medium inevitably mismatches along the other directions. Therefore, there is no perfect solid material for the ideal strain. However, although the method is not perfect, the purpose of uniaxial compression is realized at least by viewing the contrasted result between the different directions of compression. As for treatment, before it

becomes hardened, the epoxy reacts chemically against samples. It reduces the chemical bond of organic salts. For example, $(TMTSF)_2X$ salt decomposes into TMTSF and others. To protect the sample from this chemical reaction by the epoxy (Stycast 1266 and its hardener before reacted), samples are protected by coating with varnish (for example X-22 (Tamiya Inc.)) and by using the somewhat reaction-processed epoxy, which is not yet hardened.

In α-$(BEDT\text{-}TTF)_2KHg(SCN)_4$ [17] and α-$(BEDT\text{-}TTF)_2I_3$ [18], superconductivity is only realized by uniaxial compression, where BEDT-TTF is an abbreviation of bis(ethylenedithio)tetrathiafulvalene. Overlapping integrals are controlled not only by making the distance of the adjacent molecules along the stacking, but also the by making the relative angle of the molecules of adjacent columns. This angle is called a dihedral angle. In this case, transfer integral is suppressed by specific direction of compression, which gives the opposite result in contrast to the previous common examples (to the direction of conducting state). This is apparently observed as the tendency to insulate by increasing uniaxial pressure. A typical example is the θ-type conductors, where the insulating phase is charge ordered one, the θ-type conductors were developed by H. Mori [19]. The third most important role of uniaxial compression is to distort the symmetry. For instance, an equivalently interacted triangular lattice of dimers, which causes the spin of liquid down to absolute zero temperature, is broken into a non-equivalent triangular lattice by uniaxial compression. As a consequence, the spin liquid is suppressed and superconductivity is obtained [20,21]. This uniaxial technique is also applied to the research of inorganic materials.

With the development of pressure technique, lots of physics on organic conductors have developed drastically. There are already a lot of existing works with modern technique of pressure. This review is obliged to confine itself to the topics in which the authors were mainly involved.

3. TTF-TCNQ and TSeF-TCNQ

The understanding of the charge density wave (CDW) has very much progressed with the widespread and smart experiments with TTF-TCNQ. TTF donates electron to accepter TCNQ, with a charge transfer ratio of 0.59 per one pair of TTF and TCNQ. The irrational value of the charge transfer ratio of 0.59 results in an incommensurate CDW, through a relation, $\rho/a = 2/\lambda$, where ρ, a and λ are charge transfer ratio, lattice constant and the wavelength of CDW. Since incommensurate CDW is associated with a second order transition, thermodynamic fluctuation of CDW is likely, and is observed as the enhancement of excess conductivity [1,22,23] and as X-ray diffuse scattering [24–28]. The pressure gives rise to the charge transfer ratio and accordingly changes the commensurability of CDW. The ratio of 0.59 at ambient pressure increases with pressure through the commensurate value of 0.66 (= 2/3) at 1.8 GPa, where excess conductivity is suppressed. Thus the pressure work played an important role for clarifying the nature of CDW through modifying the charge transfer ratio and then the commensurability of CDW. This is the story up to 3 GPa.

The authors extended the work up to 8 GPa and obtained a *T-P* phase diagram [29], showing that the CDW is actually suppressed and a metallic state is stabilized from 300 K to helium temperature around 9 GPa, as shown in Figure 1. Superconductivity was not found at the pressure where CDW is suppressed. One possible reason for the absence of superconductivity is that the resistivity is too large for superconductivity. The suppression of CDW by pressure cannot be simply explained by the

denesting of the Fermi surface in going to higher dimension. According to S. Ishibashi, who calculated the band structure, the system becomes more 1D-like, *i.e.*, more flat Fermi surfaces seem to be realized under pressure [30]. Therefore, the role of pressure here might be to reduce the density of state though enlarging the bandwidth, which causes a reduction of the density of states. Besides the bandwidth effect, the electron correlation in the case of CDW is known to be present, specified as the presence of $4k_F$ modulation of CDW and the primary CDW of $2k_F$. The pressure effect on the correlation is an open question.

Figure 1. Temperature-Pressure phase diagram of TTF-TCNQ. Preceding work up to 3 GPa [29], including the (charge density wave) CDW commensurability peak at 1.9 GPa [31] is reproduced. The CDW is suppressed by pressure even though nesting becomes better. Reproduced with permission from JPSJ.

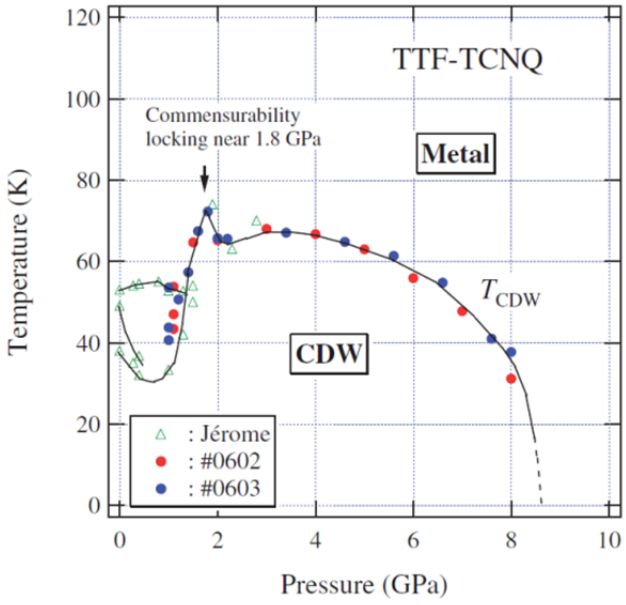

In case of tetraselenafulvalene-tetracyanoquinodimethane (TSeF-TCNQ), which is also called as TSF-TCNQ, where sulfur atoms in TTF-TCNQ are replaced with selenium, the charge transfer ratio is 0.63. We obtained *T-P* phase diagram very similar to TTF-TCNQ for TSeF-TCNQ. The metallic state is stabilized around 7 GPa [32], which is lower only by 1–2 GPa than the 8–9 GPa of TTF-TCNQ [29]. It seems that this difference is caused by the difference in the charge transfer ratio at ambient pressure, *i.e.*, 0.59 for TTF-TCNQ and 0.63 for TSeF-TCNQ. The electron correlation is much smaller in TSeF-TCNQ than TTF-TCNQ, which is confirmed by the absence of $4k_F$–CDW formation in TSeF-TCNQ, in contrast with TTF-TCNQ. But since the *T-P* phase diagram looks just shifted to lower pressure by replacing TTF- with TSeF-salt, the correlation may not play an important role in the pressure effect on CDW.

If the fluctuation of CDW is not taken into account, Soda and Jérome pointed out that the temperature dependence as well as pressure dependence of the resistivity perpendicular ($\rho_{\perp 1D}$) to the 1D axe obeys the same law as that along ($\rho_{//1D}$), *i.e.*, always $\rho_{\perp 1D}$ is proportional to the $\rho_{//1D}$ with a constant factor independent neither of pressure nor temperature, since both are dominated by a single parameter of a single electron scattering its lifetime along the 1D axis [33]. When fluctuation is

present, conductivity along the two directions shows different temperature dependence [22,23]. The present authors examined the temperature dependence of resistivity of TTF-TCNQ for various pressures up to 8 GPa [29]. It turned out that as it is at ambient pressure, the temperature dependence of resistivity for $\rho_{//1D}$ and $\rho_{\perp 1D}$ is not proportionally related. But the deviation between $\rho_{//1D}$ and $\rho_{\perp 1D}$ becomes smaller towards 8 GPa. It is concluded that when there is a CDW, there is a fluctuation. But the strength of fluctuation becomes smaller as T_{CDW} is reduced by increasing pressure [34].

4. HMTSF-TCNQ

As seen in Table 1, the stacking pattern in HMTTF-TCNQ and HMTSF-TCNQ are different from that of TTF-TCNQ and TSeF-TCNQ, where HMTTF and HMTSF stand for hexamethylenetetrathiafulvalene and hexamethylenetetraselenafulvalene. The stacking pattern is not of a layered type but of checkerboard as shown in Table 1. However, the band pictures are similar in the sense that electron and hole 1-D bands and the corresponding Fermi surface sheets are formed when the system is in the metallic state [35,36]. All of these salts undergo CDW transition. It is of interest that selenium-based TSeF-TCNQ and HMTSF-TCNQ are less electron-correlated than the sulfur-based TTF-TCNQ and HMTTF-TCNQ, which are evidenced by the absence (for non-correlated) and presence (for correlated) of $4k_F$ fluctuation of CDW viewed by X-ray.

Table 1. Comparison of four TTF-TCNQ analogues in terms of stacking pattern viewed along 1D axis, superstructures of $2k_F$ and $4k_F$, charge transfer ratio from cation to anion and the pressure, where CDW is suppressed.

	Stacking pattern (viewed along 1D)	**Super-Structure**	**Charge transfer**	P_{CDW}
TTF-TCNQ	F F F F Q Q Q Q F F F F Q Q Q Q	$2k_F$ & $4k_F$	0.59	9 GPa
TSeF-TCNQ	F F F F Q Q Q Q F F F F Q Q Q Q	$2k_F$ only	0.63	7 GPa
HMTTF-TCNQ	F Q F Q Q F Q F F Q F Q Q F Q F	$2k_F$ & $4k_F$	0.72	
HMTSF-TCNQ	F Q F Q Q F Q F F Q F Q Q F Q F	$2k_F$ only	0.74	1 GPa

The present authors revisited the HMTSF-TCNQ, and confirmed that the CDW is suppressed by a pressure of 1 GPa. In such a case where the insulating state is suppressed by pressure, the aspect of the quantum critical point in the *T*-*P* phase diagram is an attractive viewpoint. In cases when the

insulating phase of SDW is suppressed by pressure in $(TMTSF)_2X$ salts, superconductivity at low fields, field-induced SDW and quantum Hall effect at high field were observed [3]. In this case, with CDW we expected field-induced CDW when pressure was tuned at 1 GPa. Actually, magnetoresistance at 0.4 K showed some number of kink structures in the field-sweep up to 27 Tesla (sometimes to 31 Tesla) as shown in Figure 2. These kink structures are the evidence for the field-induced phase transitions, which are of first order since they accompany hysteresis [37,38]. The latest results of the present authors are; (i) Hall voltage above around 4 Tesla shows three or four steps of plateau up to 31 Tesla suggestive of quantum Hall effect. All of them are negative, but the absolute value of the Hall voltage plateau looks to be shrinking towards a higher magnetic field. This behavior is in contradiction to the usual quantum Hall effect, wherein the Hall voltage plateau should increase with an increasing field. In the case with HMTSF-TCNQ here, it might be related to the cancellation of the effect of the electrons and holes. But we note that the Hall voltage plateau levels of our result are in the same order of magnitude of h/e^2 = 25.8 kΩ. Since we were obliged to still to the phenomena at the quantum critical point in pressure, pressure was indispensable in performing this investigation. These results will be published elsewhere.

Figure 2. Magnetoresistance, which shows field-induced CDW state in HMTSF-TCNQ. Pressure at low temperature may be around 1.3 GPa at low temperature with 1.5 GPa at room temperature and with Daphne 7373 pressure medium in a piston cylinder cell [29]. Reproduced with permission from JPSJ.

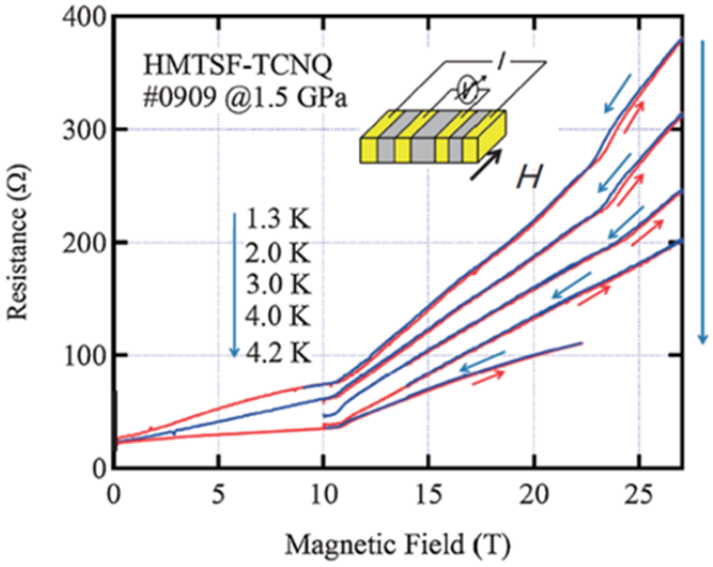

5. $(TMTTF)_2X$ and $(TMTSF)_2X$

The first organic superconductivity was found in $(TMTSF)_2PF_6$, under a pressure of 0.65 GPa at 1 K [2], and subsequently, in $(TMTSF)_2ClO_4$ at ambient pressure. $(TMTSF)_2X$ salts underwent a metal-insulator transition around 12 K, which was found to be the spin density wave (SDW) due to nesting and electron correlation. The transition from metallic to SDW states is very clear as shown by the divergence of $d(\log\rho)/dT$, where ρ is resistivity and T is temperature. The anisotropy of magnetic susceptibility of electron spins develops below T_{SDW}, which are viewed by static susceptibility [39] as well as by NMR [40,41]. In contrast to $(TMTSF)_2X$ salts, the resistivity of $(TMTTF)_2X$ also turns from

metallic to semiconductor-like temperature dependence by lowering temperature, but this "transition" is usually very dull and broad and its origin was long considered mysterious[42]. It was much later that the nature of semiconductor-like behavior was found to be originated in charge order or charge disproportionation [43–45].

Jérome proposed the generic phase diagram from $(TMTTF)_2X$ to $(TMTSF)_2X$ by the temperature as a function of pressure, locating various salts for their suitable pressure axis. The salts of $(TMTTF)_2X$ are located more left than those of $(TMTSF)_2X$ [46]. Towards the left in the Figure, the more 1D-like, charge order and spin-Peierls are there, and the antiferromagnetic states are located on the commensurate (left) side. Towards the right, the antiferromagnetic state specified as a spin density wave becomes more incommensurate, superconductivity is realized and a metallic state is stabilized. Actually, superconductivity was found in $(TMTTF)_2X$ salt by using diamond anvil cell around 5 GPa [47,48]. Later on, Itoi completed a very beautiful *T-P* phase diagram by using a cubic anvil cell as shown in Figure 3 [10]. Remarkable result was that the superconducting T_c of this family was not around 1 K, but more than 2 K for $(TMTSF)_2AsF_6$ and the superconductivity is widespread in pressure, and seems to have two T_c peaks.

Figure 3. Temperature-Pressure phase diagram of $(TMTTF)_2X$ showing that it is connected to that of the $(TMTSF)_2X$ salts. Note that the superconducting T_c is well above 2 K and spreading to a wide pressure region and the insulating phase varies from charge order to magnetic state [10]. This is the real system ,which can be compared with Jerome's generic phase diagram [46]. Reproduced with permission from JPSJ.

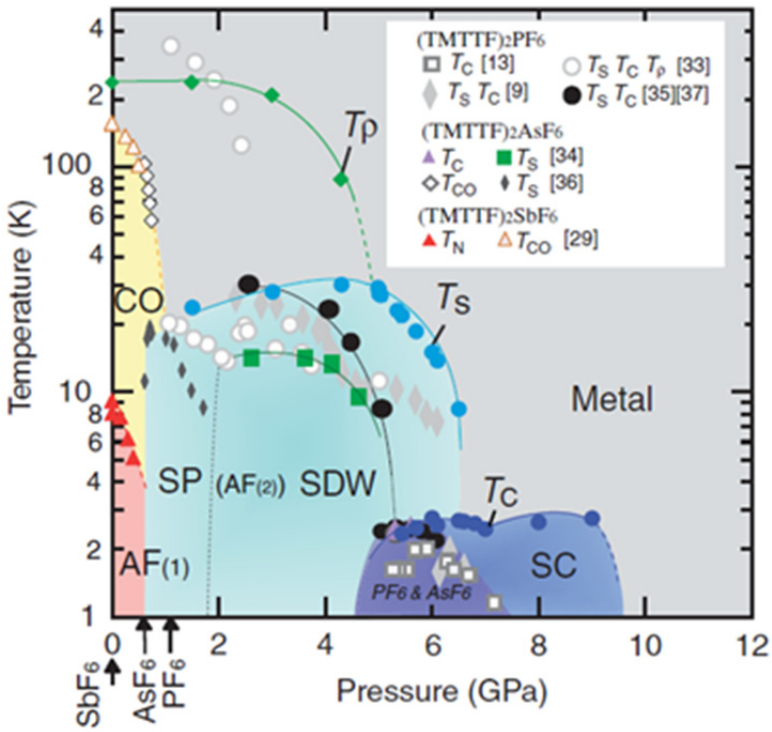

It is of interest to point out that the electron correlation plays an important role all through the Jérome's phase diagram. On the left of the diagram, charge order is the consequence of the correlation. More to the right, the SDW appears. As for the SDW, the authors examine the effect of uniaxial strain

along *a*, *b* and *c* axes on T_{SDW} in $(TMTSF)_2PF_6$. What was expected was that with *p*//*a*, the nesting becomes better; accordingly T_{SDW} might increase, whereas with either *p*//*b* or *p*//*c,* T_{SDW} might be suppressed in the same mechanism. The result differed from this expectation. The difference in T_{SDW} was very small as shown in Figure 4. This result suggests that T_{SDW} is determined not dominantly by the nesting, probably the bandwidth, density of state and electron correlation.

We note, in all directions of resistivity, ρ_a, ρ_b and ρ_c, the resistivity variation against the strain was remarkably different between *p*//*a* and other two ways, *i.e.*, *p*//*b* and *p*//*c.* That is, the resistivity reduction with *p*//*a* is as moderate as that of hydrostatic pressure, whereas with *p*//*b* or *p*//*c*, the reduction is 3–4 orders of magnitude by 1 GPa. Since only the geometrical nesting fails to explain the result as mentioned above, electron correlation effect seemed to be very dominant [49,50].

The symmetry of counter anion, X of this family, frequently plays a crucial role to material properties. When X has the inversion symmetry like octahedron with PF_6^- or AsF_6^-, an anion ordering problem does not occur. However, without the inversion symmetry like tetrahedron with ClO_4^-, ReO_4^- or BF_4^-, the orientation of tetrahedron is random at high temperature and becomes either ordered or disordered depending on cooling speed, respectively. Orientational ordering causes unit cell to be doubled and the Brillouin zone to be halved, which is called zone folding [51]. The zone folding changes the material property drastically, sometimes from metal to insulator or from superconducting to insulator. Considering that this anion ordering (AO) is available in the presence of loose space at the anion site, pressure can suppress the anion ordering, resulting as described. The present author examined the T_{AO} of $(TMTSF)_2ClO_4$ by detecting the kink in resistance up to 1.1 GPa. But the strength of anion ordering becomes very weak at 0.4 GPa [52] as shown in Figure 5.

Figure 4. Temperature-Pressure phase diagram of SDW (left-bottom region of the lines) and metal in $(TMTSF)_2PF_6$ [52]. Reproduced with permission from JPSJ.

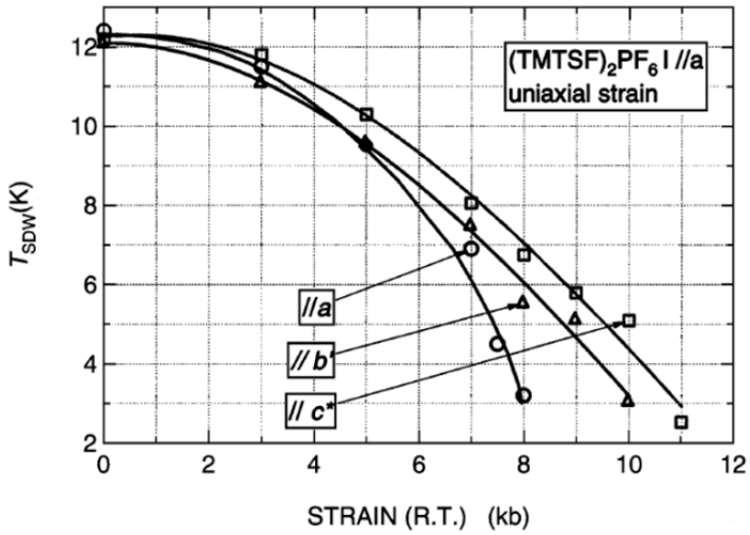

Figure 5. Temperature of anion ordering (left) and its strength (right) as a function of pressure [45]. Reproduced with permission from JPSJ.

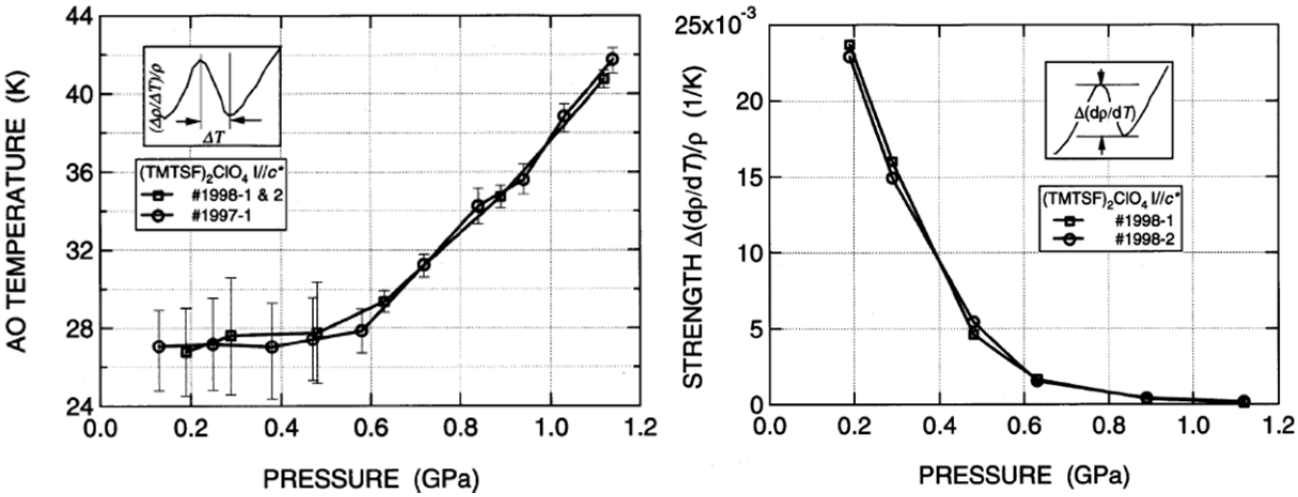

6. β-(BEDT-TTF)$_2$I$_3$

This salt is a two-dimensional conductor and showed superconductivity of 1 K at ambient pressure when it was first reported [53]. Soon after, 8 K superconductivity was reported under pressure of ~0.1 GPa independently by the present author (K/M) [54,55] and Laukhin *et al.* [56]. Historically, the discovery of the 8 K superconductivity was an important event, because many of the researchers started to move away from this field, concluding themselves that the superconducting T_c of organic crystals should not exceed much more than 1 K. At that time, the one exception was the T_c of 3 K for $(TMTSF)_2FSO_3$ [57].

The apparent existence of two T_c's as shown in Figure 6 drew attention to a new possibility. If two superconducting phases, for example, with different T_c's, coexist next to each other, it is direct evidence for non-s-wave superconductivity. In other words, the s-wave superconductivity does not have two superconducting phases. It reminded us of the two superconductivities proposed for UPt_3, where the phase boundary of two superconductivities is shown by specific measurement [58]. Later on, it was made clear that the 1 K-low T_c superconductivity is associated with an incommensurate superstructure, which appears at 195 K [59]. This superstructure is found to be suppressed by the gas pressure of 0.04 GPa [60,61], therefore, when pressure larger than 0.04 GPa is applied during cooling from room temperature through 195 K, 8 K-superconductivity is achieved even the pressure is released to zero below 195 K. As a consequence, the two phases in superconductivity supporting directly the non S-type superconductivity in terms of internal structure in superconductivity is discarded.

Application of pressure therefore simply suppresses the superconductivity. Isostructural salt like β-(BEDT-TTF)$_2$IBr$_2$ and β-(BEDT-TTF)$_2$AuI$_2$ show the superconducting T_c on the same curve of T_c *vs.* volume of β-(BEDT-TTF)$_2$I$_3$. This explains that the T_c is ruled by the density of state. Similar classification of superconducting T_c against volume was applied later for the first series of A_3C_{60}, where A and C_{60} are the alkali-element and fullerene, respectively.

As for the superconductivity, this family does not show superconductivity when the resistivity is higher than 150 μΩ·cm, which is the well-known value of the localization limit. This experiment was achieved by measuring the T_c against the residual resistivity of the various alloys, such as

β-(BEDT-TTF)$_2$(I$_3$)$_{1-x}$(IBr$_2$)$_x$, β-(BEDT-TTF)$_2$(IBr$_2$)$_{1-x}$(I$_2$Br)$_x$, β-(BEDT-TTF)$_2$(I$_2$Br)$_{1-x}$(I$_3$)$_x$ [62]. Further β-(BEDT-TTF)$_2$I$_2$Br never showed superconductivity. Among the trihalides, I$_3$, IBr$_2$ and I$_2$Br, it is known that heavy atom is located always at the center. Therefore, I$_3$ and IBr$_2$ are always symmetric, whereas I$_2$Br is always non-symmetric, which causes an orientational disorder and then becomes the source of scatterers. This is the reason for the absence of superconductivity in β-(BEDT-TTF)$_2$I$_2$Br. These series of experiments claim that the superconductivity is of a type that is weak against non-magnetic impurities.

Figure 6. Temperature-Pressure phase diagram of of β-(BEDT-TTF)$_2$I$_3$ [55]. It seemed that the two superconducting T_c's, *i.e.*, inner structure of superconductivity was suggested. However, the different series of T_c were proved related to the structure difference. Reproduced with permission from JPSJ.

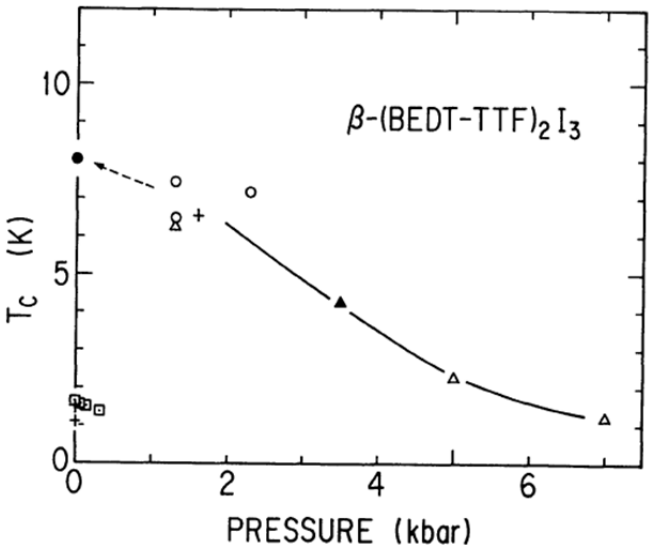

Pressure is a tool that usually reduces the electrical resistivity mainly, by the following two mechanisms: Firstly, pressure may enhance the bandwidth then mobility, in many cases. Second, pressure may enhance the dimensionality, which might help the electron pass, avoiding the scattering site. The authors tried to realized superconductivity of β-(BEDT-TTF)$_2$I$_2$Br by reducing the resistivity by means of pressure. Actually, the resistivity at room temperature was suppressed. However, the resistivity at low temperature was unchanged, which meant that the resistivity is perfectly ruled by the intrinsic and robust scatterers of I$_2$Br-anions at low temperature and by the band effect at high temperature [63]. It might be interesting to work in the future with an uniaxial strain from this view point.

Another way to approach superconductivity is whether or not the upper critical field, H_{c2} of superconductivity, is limited by the Clogston-Pauli value. This experiment was carried out under pressure with precise adjustment of the orientation of the magnetic field parallel to the 2D layer of the crystal by rotating the pressure cell in high magnetic field. The result was that the H_{c2} did not increase after lowering the temperature and looked saturated by the value of Pauli value, which supported the S-type superconductivity [64]. However, it was reported that the ambient pressure superconductivity of 7.1 K generated by the Ginodman's method [61] showed H_{c2}, which exceeded Pauli limit [65]. Therefore 8 K superconductivity achieved either by under pressure or by a special temperature-

pressure path during cooling showed different results. It might be related to the amount of scatterers due to the perfectness of the crystal, since this superconductivity is very sensitive to impurities as mentioned above.

The Fermiology by means of the Shubnikov de Haas effect of organic conductors started with this material [66–68] alongside κ-(BEDT-TTF)$_2$Cu(NCS)$_2$ [69]. Once the Fermi-surface of the 2D organic conductors is found to be the real objects, Fermiology by means of angular dependence of magnetoresistance developed Kajita-Yamaji oscillation [70–72].

7. α-(BEDT-TTF)$_2$I$_3$

This salt has a different crystal structure from β-(BEDT-TTF)$_2$I$_3$, and both α- and β-salts were found even in the same batch grown by the electrochemical method. Without using X-ray, the structural type of crystal is distinguished by the ESR bandwidth, 70–110 Gauss (20–25 Gauss) for α (for β) crystals [73–76]. Historically and technically, α and β appeared at the same time even in the same batch in the crystal growth. And β has been focused on for study because of the existence of superconductivity and its drastically high T_c of 8 K. What was found in the α-salt was that the temperature dependence of resistivity looked metallic but very weak, the sharp metal-insulator (M-I) transition occurs at 135 K, and this M-I transition is suppressed by pressure. Kajita, Tajima *et al*. studied the pressure effect up to 1.9 GPa and found that this very flat temperature dependence continuing to liquid helium temperature [77]. Their Hall effect study suggested that the carrier numbers decreased from room to helium temperature by 5–6 orders of magnitude. Much later, A. Kobayashi, Katayama *et al*. explained the temperature dependence of resistivity and Hall effect in terms of Dirac cone structure in the electronic band structure [78].

At the same time, this material shows charge disproportionation in the metallic state and charge ordering in the insulating state, which was proved by NMR chemical shift study [79], which is also true under pressure even though the T_{MI} is lowered by pressure [80]. In the Dirac cone state, the system is in the insulating state where charge ordering is established. There are two Dirac cones in the first Brillouin zone. Montambaux predicted that the two Dirac cones approaches each other by increasing pressure and merge into one where gap opens beyond 4 GPa [81]. However, Kino pointed out that pressure just make the Dirac cones more tilt and one side of the cones will make a negative slope and gap will disappear keeping the cone structure [82]. The present authors performed the high pressure measurement up to 8 GPa using cubic anvil pressure cell, which ensures constant pressure down to 2 K. Against the theoretical prediction of semiconducting behavior above 4 GPa, our result is that the almost temperature independent resistivity behavior is unchanged up to 8 GPa. Furthermore, the sheet resistance value is very close to the universal resistance of 25.8 kΩ in the temperature-independent resistivity region in Figure 7. It can be concluded that the Dirac cone electronic structure is stable under pressure at least up to 8 GPa.

Figure 7. Temperature dependence of resistivity of α-(BEDT-TTF)$_2$I$_3$ as examined by the present authors. It is obvious that the Dirac cone state is stabilized even at 8 GPa.

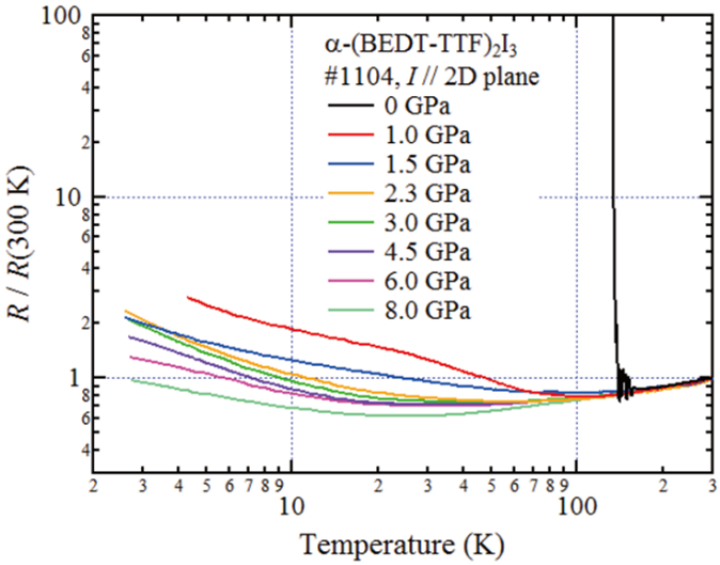

It is remarkable that the superconductivity is found under uniaxial strain along the *a*-axis, but not along the *b*-axis as shown in Figure 8. Around the superconductivity in the temperature-strain phase diagram, the charge ordered state is located. This suggested a new mechanism of superconductivity related to charge order. Historically, Dirac cone was found in graphene, the one sheet of graphite that is very fragile and hard to treat. Many of the possible experiments are still limited. From the work with α-(BEDT-TTF)$_2$I$_3$ the Dirac cones, which are of course slightly different from those of graphene, were found in a bulk system. Therefore, the research on the Dirac cone flourished.

Figure 8. Temperature-Strain phase diagram of α-(BEDT-TTF)$_2$I$_3$ [18]. Superconductivity is seen only with the strain along the *a*-axis. Around the superconductivity, charge ordered phase is located. Reproduced with permission from JPSJ.

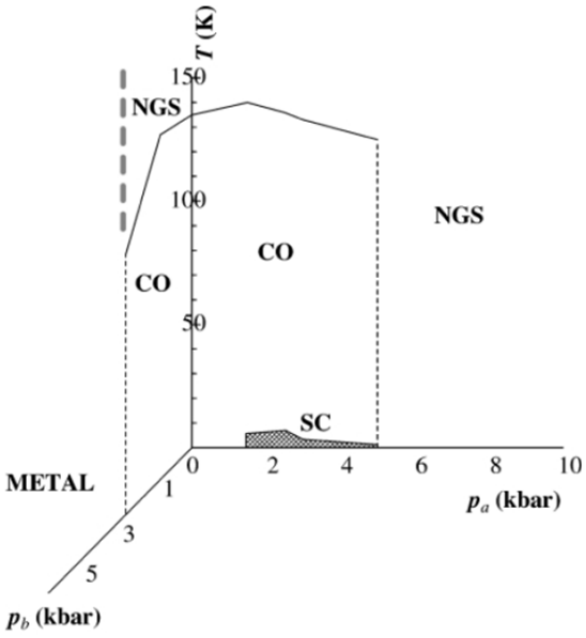

8. κ-(MeDH-TTP)$_2$AsF$_6$

The crystal of κ-type itself seems to form an inevitably dimerized structure. However, the dimerization energy in κ-(MeDH-TTP)$_2$AsF$_6$ is one order of magnitude smaller than the usual κ-type crystals. The dimerized structure is related to half-filled and then to Mott insulator. Then an interesting question arises whether the very weakly dimerized structure can induce a quarter-filled band and then charge ordered state [83]. With this interest, the temperature dependence of resistivity of κ-(MeDH-TTP)$_2$AsF$_6$ for various pressures up to 6 GPa was studied, where MeDH-TTP stands for 2-methyl-5-(1,3-dithiolan-2-yliden)-1,3,4,6-tetrathiapentalene [84]. At ambient pressure the system was completely insulating. But by increasing pressure, a metallic state appeared below room temperature, and then the metal-insulator transition became sharper. With further increase of pressure, insulating state was suppressed, and we anticipated superconductivity around 2.2 GPa. However, the system suddenly became Fermi liquid state without showing superconductivity. As shown by the phase diagram in Figure 9, the divergence of A, which is the prefactor of the T^2-term in resistivity from higher pressure to 2.2 GPa, was observed. In this way, the system showed a typical quantum critical point.

Figure 9. Temperature dependence of resistivity of κ-(MeDH-TTP)$_2$AsF$_6$ under hydrostatic pressure by cubic anvil cell with pressure medium of Daphne 7373 (top left). Temperature-Pressure phase diagram showing quantum critical point (top right). Divergence of the prefactor, A of T^2-term in resistivity and the residual resistivity (bottom) [84]. Reproduced with permission from JPSJ.

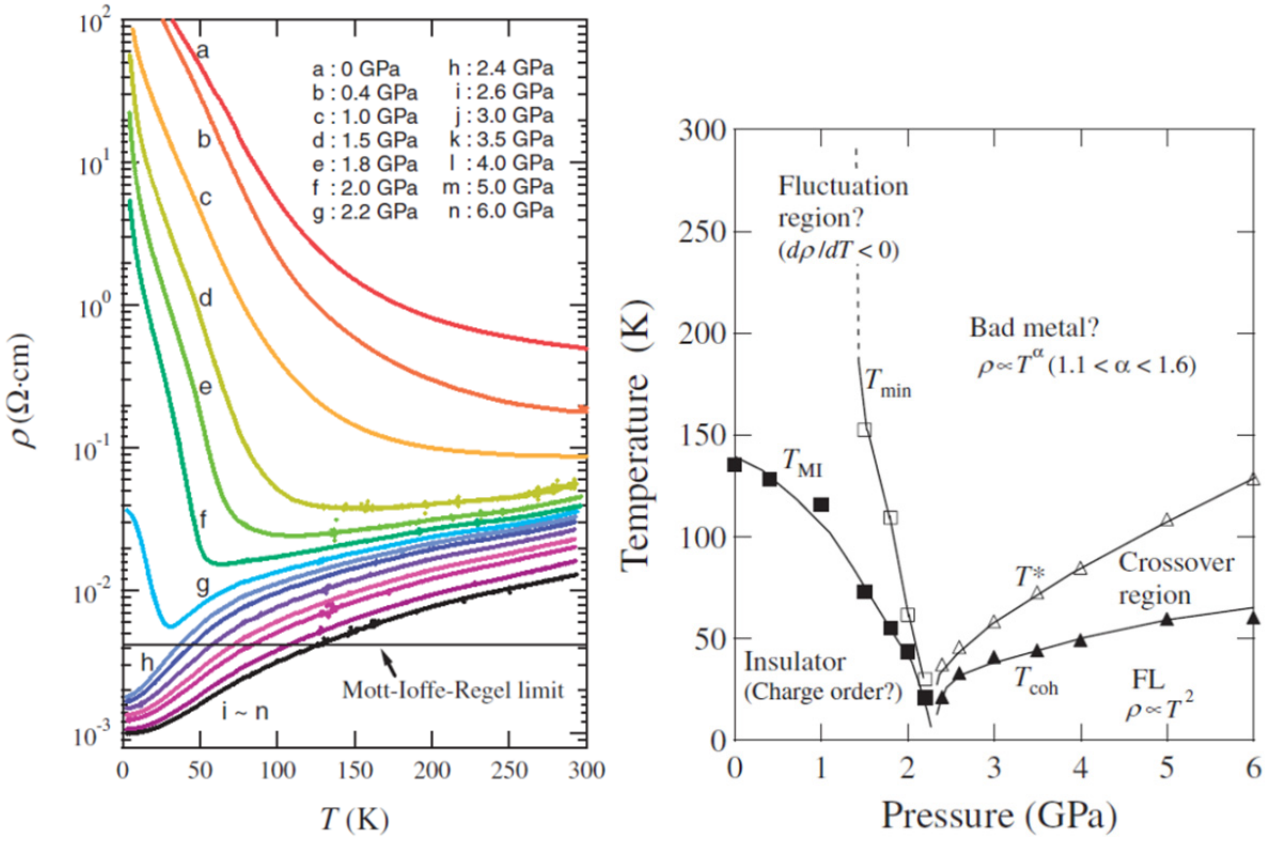

Figure 9. *Cont.*

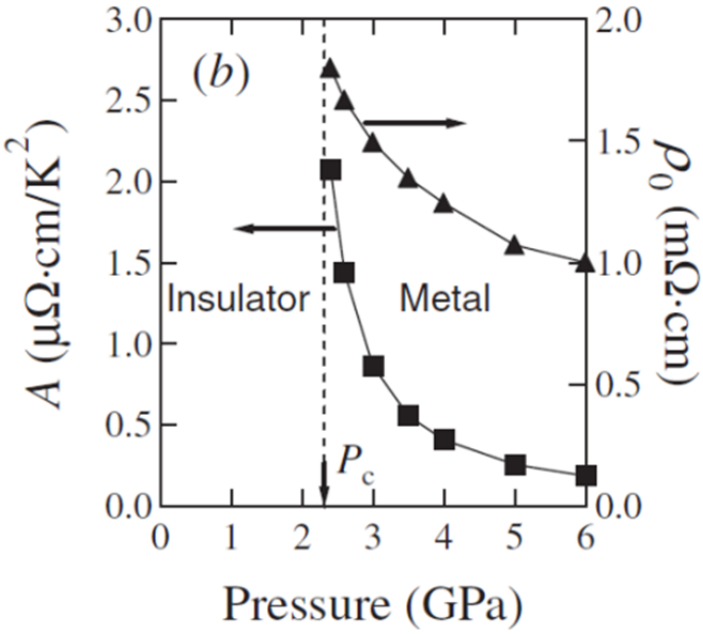

9. τ-type Conductors

The chemical formula of τ-type conductor is τ-D_2A_{1+y}, where D is a chiral donor such as P-(*S*,*S*)-DMEDT-TTF or EDO-*S*,*S*-DMEDT-TTF, and A is a linear anion such as I_3^-, $AuBr_2^-$, and *y* is around 0.75–0.9 [85,86]. The names of P-(*S*,*S*)-DMEDT-TTF or EDO-*S*,*S*-DMEDT-TTF come from pyrazino-(*S*,*S*)-dimethyl-ethylenedithio-tetrathiofulvalene and ethylenedioxy-*S*,*S*-dimethylenedithio tetrathiafulvalene, respectively. Due to the low symmetry of chiral donors, one unit cell includes four layers of D_2A_{1+y} perpendicular to the conducting plane in a chiral manner. The same anion A is located in two different typical sites; one is inside the conducting layer completely as expresses by 1 in A_{1+y}, the other is in between the layers with a deficiency as described as *y* (< 1) in A_{1+y}. Since the unit cell structure perpendicular to the conducting layer is so complicated as four-fold, the band calculation was carried out for a single layer neglecting the four-fold structure for a unit cell in the real system. The calculated electronic structure and the Fermi surface for a single sheet give a four-fold star-shaped 2D Fermi surface in a square Brillouin zone.

The positional deficiency of the trihalide-anion at the interlayer site, with which value *y* is related, is one origin of disorder. Another type of disorder comes from either the two ways of bending of the non-planar ring including two oxygen atoms in the donor EDO-*S*,*S*-DMEDT-TTF or the two ways of chirality of two methyl groups in the P-*S*,*S*-DMEDT-TTF [87]. Furthermore, anions layers in between the conducting layers make different periodicity from that of the donors. Some of the conductors exhibit superstructure below ~245 K [88].

Probably due to two types of disorder, especially due to the deficiency of the I_3-anions, which are likely to dissociate from the crystals, the temperature dependence of resistivity of τ-type conductors is very sample dependent. However, roughly speaking, all of the crystals are metallic down to 30–100 K, and show resistance upturn at low temperature. Accordingly, the resistance ratio $R_{300\ K}/R_{low\ temp}$ is almost 1, which suggests the Shubnikov de Haas (SdH) effect is unlikely. However, a very clear gigantic SdH effect is observed as shown in Figure 10 [89]. From this observation, the system has at

least a clean nature in spite of many disorders. The authors found two Fermi surface pockets, *i.e.*, 0.66% and 6.1% of the FBZ (first Brillouin zone) for τ-(EDO-*S*,*S*-DMEDT-TTF)$_2$(AuBr$_2$)$_{1+y}$, and 2.3% and 6.9% for τ-(P-*S*,*S*-DMEDT-TTF)$_2$(AuBr$_2$)$_{1+y}$ [89,90]. Both of these values are inconsistent with the value of 12.5% calculated for *y*; 0.75. The small FS pocket of 0.66% is realized the Landau quantum limit, and the larger FS plays a role of reservoir of carriers at the intermediate temperature, and quantum Hall effect is realized there (~1 K) [91]. At a lower temperature, the Landau levels of the large FS pocket separate each other, and longer the large FS pocket no longer plays as a carrier reservoir. This is the reason that lowest temperature is not suitable to observe quantum Hall effect.

Figure 10. Giant Shubnikov-de Haas oscillation in τ-(EDO-*S*,*S*-MEEDT-TTF)$_2$(AuBr$_2$)$_{1+y}$ (top), and it 1/*B*-plot (bottom) [89]. Reproduced with permission from *Physical Review B*.

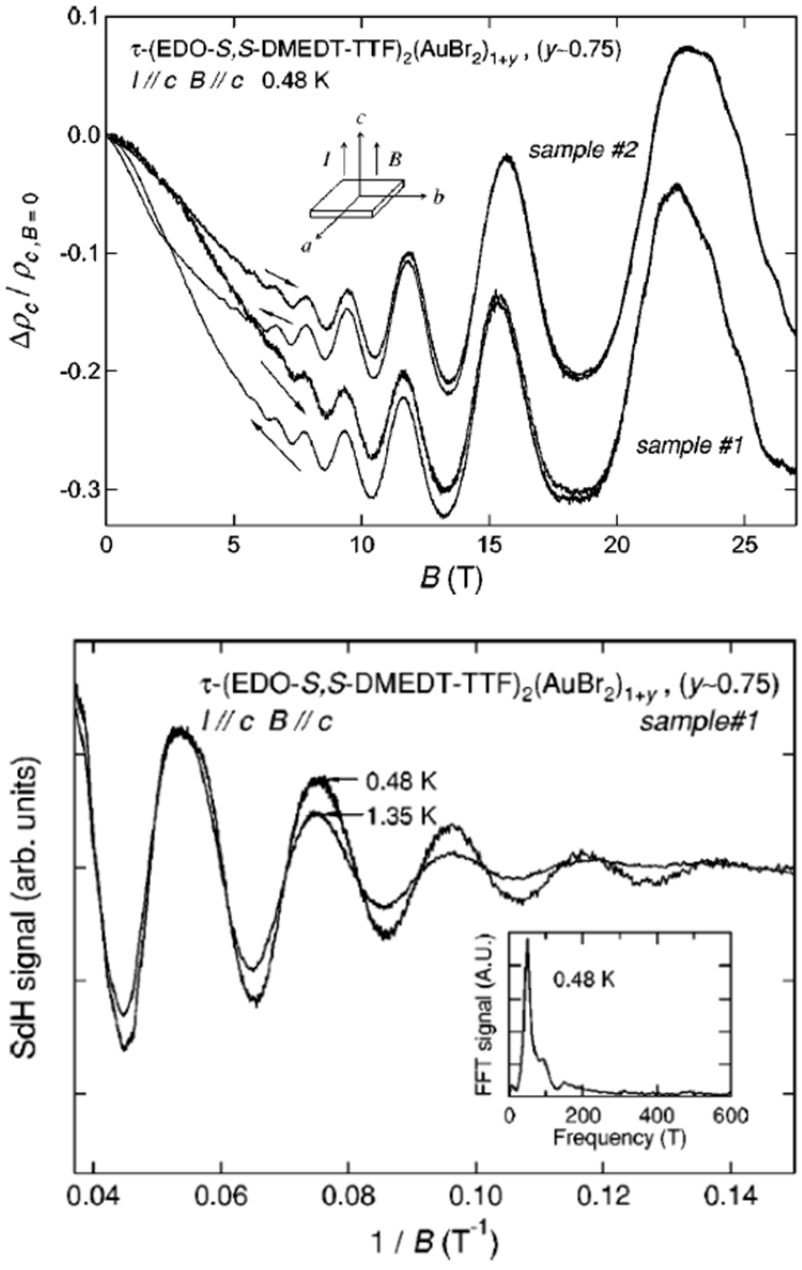

At a high field above 38 T, the system turns into a field-induced insulating state with large hysteresis [92]. The pressure effect for these materials is very striking. This field induced insulating

phase is easily suppressed by extremely low pressure, namely much smaller than 0.1 GPa. The reason is unexplained. Recently, these materials drew attention by its large thermoelectric power based on the flat band in the electronic structure [93].

10. Conclusion

We reviewed many but limited kinds of topics, as were discussed in association with pressure works on organic conducting crystals. We started with TTF-TCNQ and finished with recent materials with which the authors were deeply involved. Since covering everything was impossible, we dared to skip even some important materials such as κ-type conductors and DCNQ-materials. We also did not touch the materials that include two competing phases of charge order and Mott insulating states found in β-(BDA-TTP)$_2$I$_3$, despite these being the authors' current topics [94,95]. However, although limited subjects were treated in this paper, we believe it will be realized that how much pressure has contributed to the development of this field of organic conductors.

Acknowledgements

The part of this work was supported in part by the partially supported by the Grant-in-Aid for priority area 23110722.

References

1. Andrieux, A.; Schulz, H.J.; Jérome, D. Conductivity of the one-dimensional conductor tetrathiafulvalene-tetracyanoquinodimethane (TTF-TCNQ) near commensurability. *Phys. Rev. Lett.* **1979**, *43*, 227–230.
2. Jérome, D.; Mazaud, A.; Ribault, M.; Bechgaard, K. Superconductivity in a synthetic organic conductor (TMTSF)$_2$PF$_6$. *J. Phys. Lett*. **1980**, *41*, L95–L98.
3. Chaikin, P.M. Field Induced Spin density waves. *J. Phys. I France* **1996**, *6*, 1875–1898.
4. Wu, M.K.; Ashburn, J.R.; Torng, C.J.; Hor, P.H.; Meng, R.L.; Gao, L.; Huang, Z.J.; Wang, Y.Q.; Chu, C.W. Superconductivity at 93 K in a new mixed-phase Y-Ba-Cu-0 compound system at ambient pressure. *Phys. Rev. Lett.* **1987**, *58*, 908–910.
5. Murata, K.; Yoshino, H.; Yadav, H.O.; Honda, Y.; Shirakawa, N. Pt resistor thermometry and pressure calibration in a clamped pressure cell with the medium, Daphne 7373. *Rev. Sci. Instrum*. **1997**, *68*, 2490–2493.
6. Yokogawa, K.; Murata, K.; Yoshino, H.; Aoyama, S. Solidification of high pressure medium Daphne 7373. *Jpn. J. Appl. Phys*. **2007**, *46*, 3636–3639.
7. Shishido, H.; Ueda, T.; Hashimoto, S.; Kubo, T.; Settai, R.; Harima, H.; Onuki, Y. A de Haas–van Alphen experiment under pressure on $CeCoIn_5$, deviation from the quantum critical region. *J. Phys. Condens. Matter* **2003**, *15*, L499–L504.
8. Takashima, M.; Aoki, H.; Haworth, C.J.; Matsumoto, T.; Terashima, T.; Uji, S.; Terakura, C.; Miura, T.; Uesawa, A.; Suzuki, T. De Haas-van Alphen effect of CeSb under pressure. *J. Phys. Soc. Jpn.* **1998**, *167*, 3859–3866.

9. Taniguchi, H.; Miyashita, M.; Uchiyama, K.; Satoh, K.; Mori, N.; Okamoto, H.; Miyagawa, K.; Kanoda, K.; Hedo, M.; Uwatoko, Y. Superconductivity at 14.2 K in layered organic under extreme pressure. *J. Phys. Soc. Jpn*. **2003**, *72*, 468–471.
10. Itoi, M.; Araki, C.; Hedo, M.; Uwatoko, Y.; Nakamura, T. Anomalously wide superconducting phase of one-dimensional organic conductor $(TMTTF)_2SbF_6$. *J. Phys. Soc. Jpn*. **2008**, *77*, 1–4.
11. Murata, K.; Yokogawa, K.; Yoshino, H.; Klotz, S.; Munsch, P.; Irizawa, A.; Nishiyama, M.; Iizuka, K.; Nanba, T.; Okada, T.; Shiraga, Y.; Aoyama, S. Pressure transmitting medium Daphne 7474 solidifying at 3.7 GPa at room temperature. *Rev. Sci. Instrum.* **2008**, *79*, 1–8.
12. Kotegawa, H.; Kawazoe, T.; Sugawara, H.; Murata, K.; Tou, H. Effect of uniaxial stress for pressure-induced superconductor, $SrFe_2As_2$. *J. Phys. Soc. Jpn*. **2009**, *78*, 1–4.
13. Yamazaki, T.; Takeshita, N.; Kobayashi, R.; Fukazawa, H.; Kohori, Y.; Kihou, K.; Lee, C.H.; Kito, H.; Iyo, A.; Eisaki, H. Appearance of pressure-induced superconductivity in $BaFe_2As_2$ under hydrostatic conditions and its extremely high sensitivity to uniaxial stress. *Phys. Rev. B* **2010**, *81*, 1–5.
14. Campos, C.E.; Brooks, J.S.; van Bentum, P.J.M.; Perenboom, J.A.A.J.; Rook, J.; Klepper, S.J.; Tokumoto, M. Uniaxial stress method for delicate crystals: Application to Shubnikov-de Haas and superconductivity studies in organic conductors. *Rev. Sci. Instrum.* **1995**, *66*, 1061–1064.
15. Maesato, M.; Kaga, Y.; Kondo, R.; Kagoshima, S. Uniaxial strain method for soft crystals: Application to the control of the electronic properties of organic conductors. *Rev. Sci. Instrum.* **2000**, *71*, 176–181.
16. Kondo, R.; Kagoshima, S.; Harada, J. Crystal structure analysis under uniaxial strain at low temperature using a unique design of four-axis X-ray diffractometer with a fixed sample. *Rev. Sci. Instrum.* **2005**, *76*, 1–7.
17. Campos, C.E.; Brooks, J.S.; van Bentum, P.J.M.; Perenboom, J.A.A.J.; Klepper, S.J.; Sandhu, P.S.; Valfells, S.; Tanaka, Y.; Kinoshita, T.; Kinoshita, N.; Tokumoto, M.; Anzai, H. Uniaxial-Stress-Induced superconductivity in organic conductors. *Phys. Rev. B* **1995**, *52*, R7014–R7017.
18. Tajima, N.; Ebina-Tajima, A.; Tamura, M.; Nishio, Y.; Kajita, K. Effects of uniaxial strain on transport properties of organic conductor alpha-$(BEDT\text{-}TTF)_2I_3$ and discovery of superconductivity. *J. Phys. Soc. Jpn.* **2002**, *71*, 1832–1835.
19. Maesato, M.; Shimizu, Y.; Saito, G.; Miyagawa, K.; Kanoda, K. Spin-Liquid behavior and superconductivity in κ-$(BEDT\text{-}TTF)_2X$: The role of uniaxial strain. *J. Phys. IV France* **2004**, *114*, 227–231.
20. Mori, H.; Tanaka, S.; Mori, T. Systematic study of the electronic state in θ-type BEDT-TTF organic conductors by changing the electronic correlation. *Phys. Rev. B* **1998**, *57*, 12023–12029.
21. Shimizu, Y.; Miyagawa, K.; Kanoda, K.; Maesato, M.; Saito, G. Spin liquid state in an organic Mott insulator with a triangular lattice. *Phys. Rev. Lett.* **2003**, *91*, 1–4.
22. Andrieux, A.; Schulz, H.J.; Jérome, D.; Bechgaard, K. Fluctuation conductivity in 1-D conductor tetrathiafulvalene-tetracyanoquinodimethane (TTF-TCNQ). *J. Phys. Lett.* **1979**, *40*, L385–L389.
23. Jérome, D.; Schulz, H.J. Organic conductors and superconductors. *Adv. Phys*. **1982**, *31*, 299–490.
24. Pouget, J.-P. X-Ray diffuse scattering as precursor of incommensurate Peierls transitions in one-dimensional organic charge transfer conductors. *Z. Kristallogr. (Munich)* **2004**, *219*, 711–718.

25. Khanna, S.K.; Pouget, J.P.; Comes, R.; Garito, A.F.; Heeger, A.J. X-Ray studies of $2k_F$ and $4k_F$ anomalies in tetrathiafulvalene-tetracyanoquinodimethane (TTF-TCNQ). *Phys. Rev. B* **1977**, *16*, 1468–1479.
26. Pouget, J.-P.; Khanna, S.K.; Denoyer, F.; Comes, R.; Garito, A.F.; Heeger, A.J. X-Ray observation of $2k_F$ and $4k_F$ scatterings in tetrathiafulvalene-tetracyanoquinodimethane (TTF-TCNQ). *Phys. Rev. Lett.* **1976**, *37*, 437–440.
27. Kagoshima, S.; Ishiguro, T.; Anzai, H. X-Ray scattering study of phonon anomalies and superstructures in TTF-TCNQ. *J. Phys. Soc. Jpn*. **1976**, *41*, 2061–2071.
28. Jérome, D. Organic conductors: From charge density wave TTF-TCNQ to superconducting $(TMTSF)_2PF_6$. *Chem. Rev*. **2004**, *104*, 5565–5591.
29. Yasuzuka, S.; Murata, K.; Arimoto, T.; Kato, R. Temperature-Pressure phase diagram in TTF-TCNQ: Strong suppression of charge-density-wave state under extremely high pressure. *J. Phys. Soc. Jpn.* **2007**, *76*, 1–4.
30. Ishibashi, S.; Kohyama, M. Ab initio pseudopotential calculation for TTF-TCNQ and TSeF-TCNQ. *Phys. Rev. B* **2000**, *62*, 7839–7844.
31. Friend, R.H.; Miljak, M.; Jérome, D. Pressure dependence of the phase transitions in tetrathiafulvalene-tetracyanoquinodimethane (TTF-TCNQ): Evidence for a longitudinal lock-in at 20 kbar. *Phys. Rev. Lett.* **1978**, *40*, 1048–1051.
32. Murata, K. Temperature-Pressure phase diagram of TSeF-TCNQ. Osaka City University, Osaka, Japan. Unpublished work, 2006.
33. Soda, G.; Jérome, D.; Weger, M.; Fabre, J.M.; Giral, L. Interchain coupling and nuclear magnetic relaxation in the organic conductor tetrathiafulvalene-tetracyanoquinodimethane TTF-TCNQ. *Solid State Commun.* **1976**, *18*, 1417–1421.
34. Murata, K.; Weng, Y.; Seno, Y.; Tamilselvan, N.R.; Kobayashi, K.; Arumugam, S.; Takashima, Y.; Yoshino, H.; Kato, R. Fluctuation of the charge density wave in TTF-TCNQ under high pressure. *Phys. B Phys. Condens. Matter* **2009**, *404*, 373–375.
35. Weger, M. A model for the electronic band structure of HMTSeF-TCNQ. *Solid State Commun.* **1976**, *19*, 1149–1155.
36. Ishibashi, S. Electronic band structure calculation under pressure of TTF-TCNQ. Agency of Industrial Science and Technology, Tsukuba, Japan. Private Communication, 2008.
37. Murata, K.; Yokogawa, K.; Kobayashi, K.; Masuda, K.; Sasaki, T.; Seno, Y.; Tamilselvan, N.R.; Yoshino, H.; Brooks, J.S.; Jérome, D.; *et al*. Field-Induced successive phase transitions in the CDW organic conductor HMTSF-TCNQ. *J. Phys. Soc. Jpn.* **2010**, *79*, 1–4.
38. Murata, K.; Kang, W.; Masuda, K.; Kuse, T.; Sasaki, T.; Yokogawa, K.; Yoshino, H.; Brooks, J.S.; Choi, E.S.; Kiswandhi, A.; Kato, R. Field-Induced CDW in HMTSF-TCNQ. *Phys. B* **2012**, *407*, 1927–1929.
39. Mortensen, K.; Tomkiewicz, Y.; Bechgaard, K. Antiferromagnetism in the organic conductor, bis-tetramethyltetraselenafulvalene hexafluoroarsenate, $[(TMTSF)_2AsF_6]$: Static magnetic susceptibility. *Phys. Rev. B* **1982**, *25*, 3319–3325.
40. Takahashi, T.; Maniwa, Y.; Kawamura, H.; Saito, G. Determination of SDW characteristics in $(TMTSF)_2PF_6$ by ^{1}H-NMR analysis. *Phys. B + C* **1986**, *143*, 417–421.

41. Delrieu, J.M.; Roger, M.; Toffano, Z.; Moradpour, A.; Bechgaard, K. NMR proton lineshape in $(TMTSF)_2X$: Incommensurability of nesting vector and order parameter. *J. Phys. France* **1986**, *47*, 839–861.
42. Murata, K.; Anzai, H.; Ukachi, T.; Ishiguro, T. Metal-Insulator transition in $(TMTTF)_2BF_4$ under pressure. *J. Phys. Soc. Jpn.* **1984**, *53*, 491–494.
43. Chow, D.S.; Zamborszky, F.; Alavi, B.; Tantillo, D.J.; Baur, A.; Merlic, C.; Brown, S.E. Charge ordering in the TMTTF Family of molecular conductors. *Phys. Rev. Lett.* **2000**, *85*, 1698–1701.
44. Zamborszky, F.; Raas, W.Y.W.; Brown, S.E.; Alavi, B.; Merlic, C.A.; Baur, A. Competition and coexistence of bond and charge orders in $(TMTTF)_2AsF_6$. *Phys. Rev. B* **2002**, *66*, 1–4.
45. Takahashi, T.; Nogami, Y.; Yakushi, K. Charge ordering in organic conductors. *J. Phys. Soc. Jpn.* **2006**, *75*, 1–17.
46. Jérome, D. The physics of organic superconductors. *Science* **1991**, *252*, 1509–1514.
47. Adachi, T.; Ojima, E.; Kato, K.; Kobayashi, H.; Miyazaki, T.; Tokumoto, M.; Kobayashi, A. Superconducting transition of $(TMTTF)_2PF_6$ above 50 kbar [TMTTF = Tetramethyltetra-thiafulvalene. *J. Am. Chem. Soc.* **2000**, *122*, 3238–3239.
48. Jaccard, D.; Wilhelm, H.; Jérome, D.; Moser, J.; Carcel, C.; Fabre, J.M. From spin-Peierls to superconductivity: $(TMTTF)_2PF_6$ under high pressure. *J. Phys. Condens. Matter* **2001**, *13*, L89–L95.
49. Guo, F.Z.; Murata, K.; Oda, A.; Mizuno, Y.; Yoshino, H. Spin density wave transition in $(TMTSF)_2PF_6$ under uniaxial strain. *J. Phys. Soc. Jpn.* **2000**, *69*, 2164–2169.
50. Murata, K.; Mizuno, Y.; Guo, FZ.; Shodai, S.; Iwashita, K.; Yoshino, H. Spin density wave in a reduced anisotropy in $(TMTSF)_2PF_6$. *Mol. Cryst. Liq. Cryst.* **2002**, *380*, 85–92.
51. Grant, P.M. Electronic structure of the 2:1 charge transfer salts of TMTCF. *J. Phys. Colloques* **1983**, *44*, 847–857.
52. Guo, F.Z.; Murata, K.; Yoshino, H.; Maki, S.; Tanaka, S.; Yamada, J.; Nakatsuji, S.; Anzai, H. Anion-Ordering transition in $(TMTSF)_2ClO_4$ under pressure. *J. Phys. Soc. Jpn.* **1998**, *67*, 3000–3002.
53. Yagubskii, E.B.; Shchegolev, I.F.; Laukhin, V.N.; Kononovich, P.A.; Karatsovnik, M.V.; Zvarykina, A.V.; Buravov, L.I. Normal-Pressure superconductivity in an organic metal $(BEDT\text{-}TTF)_2I_3$. *JETP Lett.* **1984**, *39*, 12–16.
54. Murata, K.; Tokumoto, M.; Anzai, H.; Bando, H.; Saito, G.; Kajimura, K.; Ishiguro, T. Superconductivity with the onset at 8 K in β-$(BEDT\text{-}TTF)_2I_3$ under pressure. *J. Phys. Soc. Jpn.* **1985**, *54*, 1236–1239.
55. Murata, K.; Tokumoto, M.; Anzai, H.; Bando, H.; Saito, G.; Kajimura, K.; Ishiguro, T. Pressure phase diagram of the organic superconductor β-$(BEDT\text{-}TTF)_2I_3$. *J. Phys. Soc. Jpn.* **1985**, *54*, 2084–2087.
56. Laukhin, V.N.; Kostyuchenko, E.E.; Sushko, V.Y.; Shchegolev, I.F.; Yagubskii, E.B. Effect of pressure on the superconductivity of beta-$(BEDT\text{-}TTF)_2I_3$. *JETP Lett.* **1985**, *41*, 81–84.
57. Lacoe, R.C.; Wolf, S.A.; Chaikin, P.M.; Wudl, F.; Aharon-Shalom, E. Metal-Insulator transitions and superconductivity in ditetramethyltetraselenafulvalenium fluorosulfonate $[(TMTSF)_2FSO_3]$. *Phys. Rev. B* **1983**, *27*, 1947–1950.

58. Fisher, R.A.; Kim, S.; Woodfield, B.F.; Phillips, N.E.; Taillefer, L.; Hasselbach, K.; Flouquet, J.; Giorgi, A.L.; Smith, J.L. Specific heat of UPt_3: Evidence for unconventional superconductivity. *Phys. Rev. Lett*. **1989**, *62*, 1411–1414.
59. Leung, P.C.W.; Emge, T.J.; Beno, M.A.; Wang, H.H.; Williams, J.M.; Petricek, V.; Coppens, P. Novel structural modulation in the ambient-pressure sulfur-based organic superconductor β-(BEDT-TTF)$_2$I$_3$: Origin and effects on its electrical conductivity. *J. Am. Chem. Soc.* **1985**, *107*, 6184–6191.
60. Ravy, S.; Moret, R.; Pouget, J.P. Explanation of the phase diagram of beta-di[bis(ethylene-dithio)tetrathiafulvalene] triiodide based on the two configurations of the organic molecule. *Phys. Rev. B* **1988**, *38*, 4469–4480.
61. Ginodman, V.B.; Gudenko, A.V.; Kononovich, P.A.; Laukhin, V.N.; Shchegolev, I.F. Direct detection of the beta-1.5 beta-8 phase transition in beta-(ET)$_2$I$_3$. *JETP Lett.* **1986**, *44*, 673–677.
62. Tokumoto, M.; Anzai, H.; Murata, K.; Kajimura, K.; Ishiguro, T. Effect of Alloying on the superconductivity in organic metals β-(BEDT-TTF)$_2$ trihalides. *Synthet. Metal.* **1988**, *27*, A251–A256.
63. Murata, K.; Tokumoto, M.; Anzai, H.; Honda, Y.; Kinoshita, N.; Ishiguro, T.; Toyota, N.; Sasaki, T.; Muto, Y. Superconductivity of BEDT-TTF salts; (I) effect of pressure and alloying and (II) Shubnikov de Haas Effect. *Synthet. Metal.* **1988**, *27*, A263–A270.
64. Murata, K.; Toyota, N.; Tokumoto, M.; Anzai, H.; Saito, G.; Kajimura, K.; Morita, S.; Muto, Y.; Ishiguro, T. Upper critical field of β-(BEDT-TTF)2I3 in the High T_c superconducting state. *Phys. B* **1986**, *143*, 366–368.
65. Laukhin, V.N.; Pesotskii, S.I.; Yagubskii, E.B. Exceeding the paramagnetic limit of H_{c2} in an organic superconductor beta-(ET)$_2$I$_3$ with T_c = 7.1 K. *JETP Lett.* **1987**, *45*, 501–504.
66. Murata, K.; Toyota, N.; Honda, Y.; Sasaki, T.; Tokumoto, M.; Bando, H.; Anzai, H.; Muto, Y.; Ishiguro, T. Magnetoresistance in β-(BEDT-TTF)$_2$I$_3$ and β-(BEDT-TTF)$_2$IBr$_2$, Shubnikov de Haas effect. *J. Phys. Soc. Jpn.* **1988**, *57*, 1540–1543.
67. Toyota, N.; Sasaki, T.; Murata, K.; Honda, Y.; Tokumoto, M.; Bando, H.; Anzai, H.; Ishiguro, T.; Muto, Y. Cyclotron mass and Dingle temperature of conduction electrons moving in a layered plane of organic superconductors β-(BEDT-TTF)$_2$IBr$_2$, β-(BEDT-TTF)$_2$I$_3$ and κ-(BEDT-TTF)$_2$Cu(NCS)$_2$. *J. Phys. Soc. Jpn.* **1988**, *57*, 2616−2619.
68. Kang, W.; Montambaux, G.; Cooper, J.R.; Jérome, D.; Batail, P.; Lenoir, C. Observation of giant magnetoresistance oscillation in the high-T_c phase of the two-dimensional organic conductor beta-(BEDT-TTF)$_2$I$_3$. *Phys. Rev. Lett.* **1989**, *62*, 2559–2562.
69. Oshima, K.; Mori, T.; Inokuchi, H.; Urayama, H.; Yamochi, H.; Saito, G. Shubnikov-de Haas effect and Fermi surface in an ambient pressure organic superconductor (BEDT-TTF)$_2$Cu(NCS)$_2$. *Phys. Rev. B* **1988**, *38*, 938–941.
70. Kajita, K.; Nishio, Y.; Takahashi, T.; Sasaki, W.; Kato, R.; Kobayashi, H.; Kobayashi, A.; Iye, Y. A new type oscillatory phenomenon in the magnetotransport of θ-(BEDT-TTF)$_2$I$_3$. *Solid State Commun.* **1989**, *70*, 1189–1193
71. Yamaji, K. On the angle dependence of the magnetoresistance in quasi-two-dimensional organic superconductors. *J. Phys. Soc. Jpn.* **1989**, *58*, 1520–1523.

72. Kartsovnik, M.V.; Kononovich, P.A.; Laukhin, V.N.; Schegolev, I.F. Anisotropy of magnetoresistance and the Shubnikov-de Haas oscillations in the organic metal beta-$(ET)_2IBr_2$ *Pis'ma Zh. Eksp. Teor. Fiz.* **1988**, *48*, 498–501.
73. Hennig, I.; Bender, K.; Schweitzer, D.; Dietz, K.; Endres, H.; Keller, H.J.; Gleitz, A.; Helberg, H.W. Alpha- and beta-(BEDT-TTF)$^{2+}I^{3-}$ two dimensional organic metals. *Mol. Cryst. Liq. Cryst.* **1985**, *11*, 337–441.
74. Kinoshita, N.; Tokumoto, M.; Anzai, H.; Saito, G. Anisotropy in ESR 9 Factors and Linewidths for α-and β-$(BEDT\text{-}TTF)_2I_3$. *J. Phys. Soc. Jpn*. **1985**, *54*, 4498–4501.
75. Sugano, T.; Saito, G.; Kinoshita, M. Spin relaxation and diffusion in quasi-two-dimensional organic metals: The bis(ethylenedithiolo)tetrathiafulvalene compounds β-$(BEDT\text{-}TTF)_2X$ (X = I_3 and IBr_2). *Phys. Rev. B* **1987**, *35*, 6554–6559.
76. Sugano, T.; Saito, G.; Kinoshita, M. Conduction-Electron-Spin resonance in organic conductors: α and β phases of di[bis(ethylenedithiolo)tetrathiafulvalene]triiodide [$(BEDT\text{-}TTF)_2I_3$]. *Phys. Rev. B* **1986**, *34*, 117–125.
77. Kajita, K.; Ojiro, T.; Fujii, H.; Nishio, Y.; Kobayashi, H.; Kobayashi, A.; Kato, R. Magnetotransport phenomena of α-Type $(BEDT\text{-}TTF)_2I_3$ under high pressures. *J. Phys. Soc. Jpn.* **1992**, *61*, 23–26.
78. Katayama, S.; Kobayashi, A.; Suzumura, Y. Pressure-Induced zero-gap semiconducting state in organic conductor α-$(BEDT\text{-}TTF)_2I_3$ salt. *J. Phys. Soc. Jpn.* **2006**, *75*, 1–6.
79. Takahashi, T.; Nogami, Y.; Yakushi, K. Charge ordering in organic conductors. *J. Phys. Soc. Jpn.* **2006**, *75*, doi: 10.1143/JPSJ.75.051008.
80. Takano, Y.; Hiraki, K.; Takada, Y.; Yamamoto, H.M.; Takahashi, T. Local spin susceptibility characteristic of zero-gap state of α-$(BEDT\text{-}TTF)_2I_3$ under pressure. *J. Phys. Soc. Jpn.* **2010**, *79*, 1–7.
81. Montambaux, G.; Piéchon, F.; Fuchs, J.-N.; Goerbig, M.O. Merging of Dirac points in a two-dimensional crystal. *Phys. Rev. B* **2009**, *80*, 1–4.
82. Kino, H. Theoretical electronic band structure of alpha-$(BEDT\text{-}TTF)_2I_3$. National Research Institute for Metals, Tsukuba, Japan. Private Communication, 2012.
83. Nishikawa, H.; Sekiya, H.; Fujiwara, A.; Kodama, T.; Ikemoto, I.; Kikuchi, K.; Yamada, J.; Oshio, H.; Kobayashi, K.; Yasuzuka, S.; Murata, K. Molecular conductor based on reduced π-system donor: Insulating state of $(MeDH\text{-}TTP)_2AsF_6$. *Chem. Lett.* **2006**, *35*, 912–913.
84. Yasuzuka, S.; Kobayashi, K.; Nishiwaka, H.; Yoshino, H.; Murata, K. Quantum criticality in reduced pi-donor system $(MeDH\text{-}TTP)_2AsF_6$. *J. Phys. Soc. Jpn.* **2006**, *75*, 1–4.
85. Zambounis, J.S.; Pfeiffer, J.; Papavassiliou, G.C.; Lagouvardos, D.J.; Terzis, A.; Raptoupoulou, C.P.; Delhaes, P.; Ducasse, L.; Fortune, N.A.; Murata, K. Structural and physical properties of τ-(P-(*S*,*S*)-$DMEDT\text{-}TTF)_2(AuBr_2)_1(AuBr_2)_{0.75}$. *Solid State Commun.* **1995**, *95*, 211–215.
86. Papavassiliou, G.C.; Lagouvardos, D.J.; Zambounis, J.S.; Terzis, A.; Raptopoulou, C.R.; Murata, K.; Shirakawa, N.; Ducasse, L.; Delhaes, P. Structural and physical properties of τ-(EDO-*S*,*S*-$DMEDT\text{-}TTF)_2(AuBr_2)_1(AuBr_2)_y$. *Mol. Cryst. Liq. Cryst.* **1996**, *285*, 83–88.
87. Murata, K.; Yoshino, H.; Tsubaki, Y.; Papavassiliou, G.C. Hysteretic magnetic state in the organic τ-phase conductors. *Synthet. Metal.* **1998**, *94*, 69–72.

88. Konoike, T.; Iwashita, K.; Nakano, I.; Yoshino, H.; Sasaki, T.; Takahashi, T.; Nogami, Y.; Brooks, J.S.; Graf, D.; Mielke, C.H.; Papavassiliou, G.C.; Murata, K. Shubnikov-de Haas oscillations and low temperature electric structure in τ-phase conductors. *Synthet. Metal.* **2003**, *135–136*, 615–616.
89. Konoike, T.; Iwashita, K.; Yoshino, H.; Murata, K.; Sasaki, T.; Papavassiliou, G.C. Shubnikov de Haas oscillations in a 2D organic conductor tau-(EDO-*S*,*S*-DMEDT-TTF)$_2$(AuBr$_2$)$_{1+y}$ ($y \sim 0.75$), *Phys. Rev. B* **2002**, *66*, 1–5.
90. Storr, K.; Balicas, L.; Brooks, J.S.; Graf, D.; Papavassiliou, G.C. Magnetic-Field-Dependent interplay between incoherent and Fermi liquid transport mechanisms in low-dimensional τ-phase organic conductors. *Phys. Rev. B* **2001**, *64*, 1–9.
91. Murata, K.; Yoshino, H.; Nakanishi, T.; Konoike, T.; Brooks, J.; Graf, D.; Mielke, C.; Papavassiliou, G.C. A new quantum hall effect in the two-dimensional organic conductor, tau-(EDO-*S*,*S*-DMEDT-TTF)$_2$(AuBr$_2$)$_{1+y}$. *Curr. Appl. Phys.* **2004**, *4*, 488–490.
92. Brooks, J.S.; Graf, D.; Choi, E.S.; Balicas, L.; Storr, K.; Mielk, C.H.; Papavassiliou, G.C. High magnetic field-induced insulating phase in an organic conductor. 2002, arXiv:cond-mat/0209592v1. Available online: http://arxiv.org/abs/physics/0402096 (accessed on 9 October 2012).
93. Yoshino, H.; Aizawa, H.; Kuroki, K.; Anyfantis, G.C.; Papavassiliou, G.C.; Murata, K. Thermoelectric figure of merit of τ-type conductors of several donors. *Physica B* **2010**, *405*, S79–S81.
94. Kikuchi, K.; Isono, T.; Kojima, M.; Yoshimoto, H.; Kodama, T.; Fujita, W.; Yokogawa, K.; Yoshino, H.; Murata, K.; Kaihatsu, T.; Akutsu, H.; Yamada J. Uniaxial strain orientation dependence of superconducting transition temperature (T_c) and critical superconducting pressure (P_c) in β-(BDA-TTP)$_2$I$_3$. *J. Am. Chem. Soc.* **2011**, *133*, 19590–19593.
95. Nuruzzaman, M.; Yokogawa, K.; Yoshino, H.; Yoshimoto, H.; Kikuchi, K.; Kaihatsu, T.; Yamada, J.; Murata, K. Uniaxial-Strain-Orientation dependence of the competition between Mott and charge ordered phases and their corresponding superconductivity of β-(BDA-TTP)$_2$I$_3$. *J. Phys. Soc. Jpn*. **2012**, in press.